Asociación Argentina
de Mecánica Computacional

Mecánica Computacional Vol XLII, pp. 765-774
A. Caggiano, G. Etse, P. Folino, M. Goldschmit, M. Pucheta, M. Storti (Eds.)
S. Giusti, J. Mroginski, P. Sánchez (Issue eds.)
Buenos Aires, November 11-14, 2025

INVESTIGATING PRECURSORS IN COMPLEX SYSTEMS: INSIGHTS FROM THE FIBER BUNDLE MODEL AND THE 2017 MÉXICO MW8.2 EARTHQUAKE

Mariana H. Padilha[a], Leandro F. Friedrich[a], Ignacio Iturrioz[b] and Luis E. Kosteski[c]

[a] *Machines, Materials and Manufacturing Processes Research Group (GPMAT-PF), Universidade Federal do Pampa, Alegrete, Brazil.* marianapadilha.aluno@unipampa.edu.br; leandrofriedrich@unipampa.edu.br

[b] *Applied Mechanics Research Group (GMAP), Universidade Federal do Rio Grande do Sul, Porto Alegre, Brazil.* ignacio@mecanica.ufrgs.br

[c] *Composites Modeling and Experimental Analysis Research Group (MAEC), Universidade Federal do Pampa, Alegrete, Brazil.* luiskosteski@unipampa.edu.br

Keywords: *b*-value; Acoustic Emission; Earthquake precursors; Fiber Bundle Model; Lattice Discrete Element Method; Method of Critical Fluctuations.

Abstract. Complex systems are characterized by self-organization, where interactions among constituent elements give rise to emergent patterns and critical transitions. In geophysics, earthquakes can be interpreted within this framework, where the analysis of precursor parameters provides critical insights into impending systemic instabilities. Among these, the temporal evolution of the *b*-value, derived from the Gutenberg-Richter frequency-magnitude scaling law, serves as a principal metric, with strong parallels drawn to Acoustic Emission (AE) studies in material failure. This work investigates critical-state precursors in two complementary case studies. The first employs AE time series generated from Fiber Bundle Model (FBM) simulations implemented via a Lattice Discrete Element Method (LDEM), enabling the characterization of progressive fracture and failure. The second examines the seismic sequence preceding the Mw 8.2 earthquake that struck Mexico in 2017. In both cases, the *b*-value and the Method of Critical Fluctuations (MCF-B) are applied to track the evolution of criticality. Results demonstrate that b-value variations consistently capture the transition to a critical regime, both in simulated and real seismic data. In contrast, MCF-B shows limited applicability in complex tectonic settings dominated by large, isolated events. These findings highlight the robustness of *b*-value analysis as a precursor, while also indicating the need for refining complementary approaches. The multiscale perspective adopted here contributes to advancing the identification of critical states in both acoustic and seismic domains, with implications for earthquake forecasting.

ISSN: 2591-3522 DOI: 10.70567/mc.v42.ocsid8354

1 INTRODUCTION

Complex systems — whether physical, biological, social, or economic, consist of many elements sufficiently similar in nature for interactions to occur. Such systems are inherently open, exchanging information with their environment, and continuously reorganizing their internal structure through self-organization (Kwapien and Drozdz, 2012; Ladyman, Lambert and Wiesner, 2012). Self-organization is the spontaneous emergence of order and complexity from system–environment interactions, arising from non-equilibrium processes where external perturbations drive a stable system into a new dynamic state.

The Earth's crust can be regarded as a self-organizing complex system, where earthquakes arise from its deformation through the formation and propagation of faults. One of the fundamental relations derived from this assumption is the Gutenberg–Richter law for the frequency–magnitude distribution of earthquakes (Turcotte and Malamud, 2002). The constant b, or *b-value*, varies regionally and evolves as a major seismic event approach, making it a precursor in earthquake prediction. A parallel can be drawn with Acoustic Emission (AE) analysis, where the *b-value* acts as a precursor that signals imminent material failure, typically approaching a value close to one. AE is defined as the release of elastic waves due to the redistribution of internal stress caused by structural changes (Huang et al., 1998).

AE events can be interpreted as microscale earthquakes, since they originate from localized energy release during microcrack formation. Both AE and seismicity involve the analysis of elastic wave emissions, but they operate at different scales and frequency ranges: AE signals typically range from 20 kHz to 1 MHz, whereas seismic data occur around 1 Hz. Despite these differences, several precursor parameters have been successfully applied to both AE and seismic data (Lei and Ma, 2014).

Within this framework, the present study investigates critical-state precursors in complex systems through two case studies. The first involves AE time series from the fracture process of a fiber bundle model (FBM), implemented using a discrete element method variant known as the lattice discrete element method (LDEM). The second case study examines seismic data from the Mw 8.2 earthquake that occurred in Mexico in 2017.

2 THEORICAL BACKGROUND

2.1 The fiber bundle model

FBM is a framework for studying failure processes in heterogeneous materials, consisting of a bundle of parallel brittle, linear elastic fibers subjected to quasi-static stretching between rigid supports. As loading progresses, weaker fibers fail and stress redistribution may trigger cascades of further failures, or avalanches, analogous to amplitude distributions in AE signals or seismic data. As the stretching continues, the system eventually collapses completely (Pradhan et al., 2010).

The relation between the number of fibers breaking and the statistical distribution of events follows power-law behavior when the system is driven up to the critical threshold $x_e = x_c$, a characteristic of critical phenomena, whereas premature interrupting of loading ($x_e < x_c$) yields incomplete avalanches and a normalized distribution $N(A)/N$ that deviates from a pure power law, incorporating exponential components represented by the correction function G(Y), defined as:

$$Y = A^{\eta}(x_c - x_e) \tag{1}$$

when x_e is far from x_c, it results in $Y \gg 0$, and $G(Y) = e^{-Y}$, then a power and exponential function govern the behavior of the statistical distribution of event sizes $N(A)/N$. When x_e

approaches x_c, $G(Y)$ tends to unity, and a power law takes place. Pradhan et al. (2005) identified this deviation as a crossover phenomenon, indicating that the system is nearing a critical state where failure becomes unstable. Detecting this behavior provides an early warning signal for structural failure, making it crucial for predictive modeling in materials science and seismology.

2.2 The Lattice Discrete Element Method (LDEM)

The LDEM represents the continuum medium as elements that bear only axial loads. The discretization utilizes a cubic module, comprising twenty-six bars and nine nodes, with the total mass concentrated at the nodes. Each node possesses three degrees of freedom. The lengths of the longitudinal and diagonal elements are shown in equations 2 and 3, respectively, with L as the module length.

$$L_n = L \tag{2}$$

$$Ld = (\sqrt{3}/2)\, L \tag{3}$$

The correlation between bar properties and the elastic constants of an isotropic medium is given by explicit relations (see Kosteski et al., 2012), which define the equivalent cross-sectional areas of longitudinal and diagonal bars. Using this approach, the following equation of motion can be derived:

$$M_{ij}\ddot{x}_j + C_{ij}\dot{x}_j + F_i(t) - P_i(t) = 0 \tag{4}$$

where the vectors $\ddot{x}_j$ and $\dot{x}_j$ represent the nodal acceleration and velocity, respectively. M_{ij} represents the mass matrix, whereas C_{ij} denotes the damping matrix. The vectors $F_i(t)$ and $P_i(t)$ are the internal and external nodal forces, respectively. Since the matrices M_{ij} and C_{ij} are diagonal, Eq. (4) is not coupled and can be integrated in the time domain by using an explicit integration scheme, such as the Central Difference Method.

For fracture analysis, a bilinear constitutive law of Hillerborg (1978) is used, defining a triangular force-strain relation for the bars to capture crack nucleation and propagation under tension. The material is assumed to behave as linear elastic in compression, with failure induced by indirect tension. The key parameters of this law — the critical strain at damage initiation ε_p and the ultimate strain at failure ε_u — are derived from the material's fracture energy G_f and characteristic length d_{eq}, and can be computed by means of the following equations:

$$\varepsilon_p = \sqrt{\frac{G_f}{E d_{eq}}} \tag{5}$$

$$\varepsilon_u = K_r \varepsilon_p \tag{6}$$

where:

$$K_r = d_{eq}\left(\frac{A_i^*}{A_i}\right)\left(\frac{2}{L_i}\right) \tag{7}$$

being the parameters $\frac{A_i^*}{A_i} = 0.134$ and L_i is the bar length, the subscript i is equal to n for longitudinal bar, and equal to d for a diagonal bar. A notable feature of the LDEM is the capability to implement three-dimensional stochastic fields for material properties such as fracture energy (G_f) and elastic modulus (E). This allows for the incorporation of the material's intrinsic inhomogeneity into the model, which is crucial for simulating realistic fracture processes.

3 PRECURSOR PARAMETER

3.1 *b*-value

Gutenberg and Richter (1949) described the frequency-magnitude relation of earthquakes by the Gutenberg-Richter (G-R) law,

$$N(\geq A) = cA^{-b} \tag{8}$$

where A is the amplitude of AE signals, $N(\geq A)$ the cumulative number of signals with amplitudes ≥A, and c and b are region-dependent constants. This formulation has been successfully applied to acoustic emission (Carpinteri, 2008), highlighting the analogy between structural damage and seismicity. In this context, the *b*-value, defined as the slope linking amplitude and cumulative events, reflects the damage evolution: in early loading stages, when microcracks nucleate uniformly, $b \approx 1.5$-2; near collapse, as cracks concentrate around the failure surface, *b* decreases towards 1.

3.2 A precursor approach based on method of critical fluctuations

The Method of Critical Fluctuations Based (MCF-B) is based on the original MCF employed by Contoyiannis and Diakonos (2000) for analyzing critical fluctuations near equilibrium phase transitions. It employs a function with power-law and exponential term to capture deviations from linearity in the AE frequency-magnitude distribution, expressed as:

$$N(A) = p_1 \cdot A^{-p_2} \cdot e^{-Ap_3} \tag{9}$$

being p_1 a constant, p_2 a power-law decay exponent and p_3 an exponential decay exponent. Both p_2 and p_3 can consider deviations from data linearity in the same way as in the original MCF and therefore this proposed approach is called "based".

Monitoring the exponents p_2 and p_3 reveals the loss of linearity in the AE data and its relation to imminent collapse. Criticality emerges from their evolution in the amplitude distribution: near failure, the system shows a perfect power law with $p_2 > 1$ and $p_3 \approx 0$, followed by the decrease of p_2 and the monotonic increase of p_3, analogous to the crossover phenomenon discussed in Section 2.

4 CASE STUDY I: FBM IN THE LDEM FRAMEWORK

4.1 Model description

The LDEM consists of a cubic module with length L assumed to be equal to 1 m, represented in Fig. 1. There are 15,000 modules in horizontal direction (x-axis), 4 modules in the vertical direction (y-axis), and 1 module in the thickness direction (z-axis).

A displacement in in y-direction, u_y, is applied increasing with a velocity of $1(10)^{-7} m/s$ at the upper nodes of the model. The support is modelled as isotropic and homogeneous material; therefore, damage is not allowed in such region. The properties assumed for the LDEM support region are: $E = 1.0\ N/m^2$, $\nu = 0.25, and\ \rho = 1.0\ kg/m^3$, representing a stiffer region compared to the fibers.

Some bars of the lower module are deactivated to ensure that only a single bar is loaded, to simulate a faithful FBM. The stiffness is equal to $k = 0.4\ N/m$ for the active bars. To consider the material heterogeneity, the rupture displacement of such bars, u_r, is considered as random parameter characterized with a Weibull distribution with a mean value, $\mu\ (u_r) = 0.066\ m$, and Coefficient of Variation, $CVu_r = 50\ \%$. It is important to note that the rupture of the bars is assumed to be perfectly brittle. It is important to emphasize that the purpose of this model is

not to replicate specific materials or structures, but rather to provide a simplified representation of the behavior of the precursors under investigation.

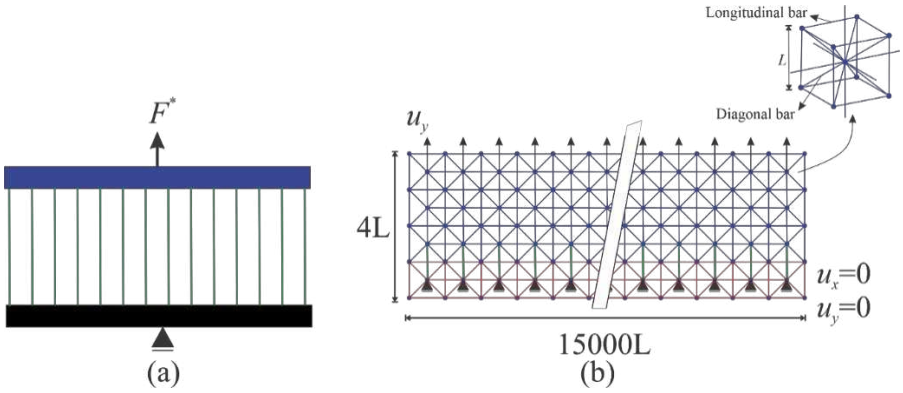

Figure 1. (a) The FBM — parallel fibers are placed between two rigid supports and are stretched by applying a force at the upper support and fixed at the lower one. (b) The FBM in the LDEM framework — bars are vertically stretched using a prescribed displacement. Detail of the LDEM cubic module.

This work introduces a novel approach by embedding the FBM within the LDEM framework, allowing for a dynamic representation of failure processes. Unlike traditional FBM applications, which analyze avalanches in a quasi-static manner, the present study incorporates time integration of the equations of motion.

This feature detects avalanches through AE events. Two strategies for monitoring AE in LDEM are considered: the derivative of the system's kinetic energy and the acceleration of a node acting as a virtual sensor. The kinetic energy approach provides a global perspective, capturing the total energy released during major failure events and supporting the monitoring of damage propagation and large-scale rupture. Node acceleration offers a localized indicator of abrupt changes, making it particularly sensitive to micro-failure dynamics. In this study, AE time series are extracted from the temporal derivative of the kinetic energy, computed in equation (10), where E_k is the kinetic energy evaluated at discrete time steps during the simulation.

$$\Delta E_k = E_k(t_i) - E_k(t_{i-1}) \tag{10}$$

4.2 Results and discussion

The accumulated number of AE events (822 have been recorded) against the normalized time (t/t_{max}, being t_{max} the time of the peak load) are presented in Fig. 2(a) together with the normalized (right-hand scale) AE amplitude and the load (the peak load, F_{max}, is equal to 182.28 N). A quantitative analysis of the accumulated number of events was conducted. It has been observed that the number of events increases at a nearly uniform rate to the point of imminent collapse.

As shown in Fig. 2(b), the energy balance calculated during the simulation is represented by the multiplication of the kinetic energy by a factor of 10^4, a technique employed to enhance the clarity of the visualization. The amplitude of the AE events, obtained from the derivative of kinetic energy, represents a spasmodic process with large amplitude AE events distributed throughout the failure process of the model. The following are typical characteristics that have been observed during experimental monitoring of real materials.

Figure 2(c) illustrates the temporal evolution of the *b*-value during the LDEM simulation, evaluated throughout the FBM simulation. At the early stages of loading, when nucleation of cracks dominates, *b*-values are between 1.5 and 2. When collapse is imminent, *b*-value

decreases towards 1. This behavior is consistent with the study by Carpinteri et al. (2008).

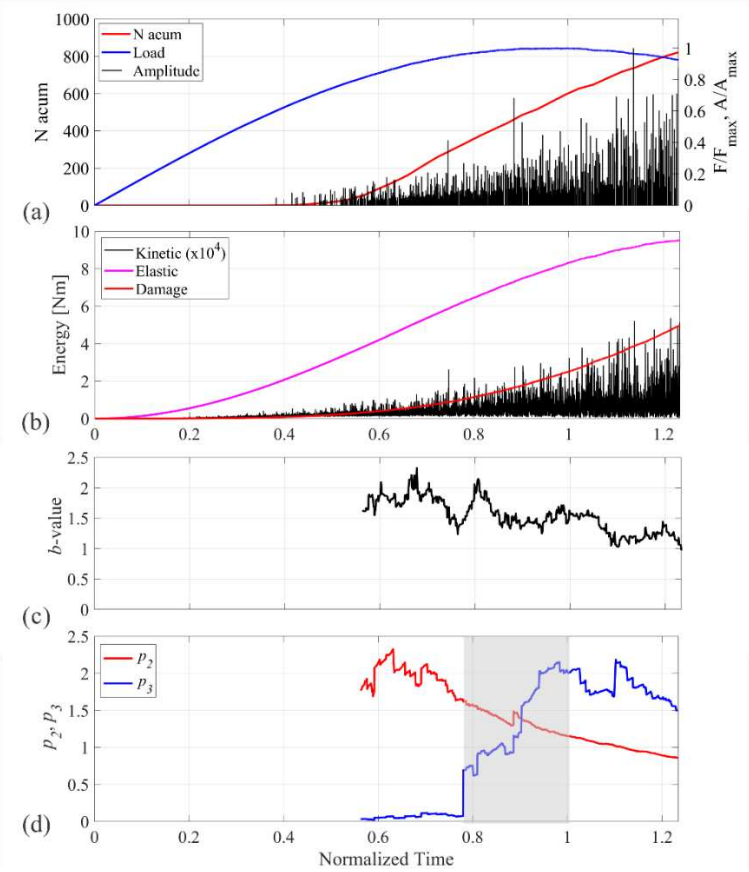

Figure 2. (a) Accumulated number of AE signals with the normalized (on the right-hand scale) load and AE-signal amplitudes; (b) Energy balance presented during the simulation; (c) b-value analysis; (d) exponents p_2 and p_3 from the MCF-B approach. The horizontal axis is the normalized time and equal for (a)-(d).

The results of applying the MCF-B approach to the AE time series from the LDEM simulation are shown in Fig. 2(d). The exponents p_2 and p_3 are calculated starting with an initial dataset of 50 AE signals and then updated event by event throughout the normalized test period. It should be recalled that the characteristic signature of the MCF-B approach, indicating that the system has reached a critical stage, is the presence of a "perfect" power law together with a simultaneous decrease of p_2 and a continuous increase of p_3. Following this definition, one critical region is identified and highlighted with a grey background in Fig. 2(d), suggesting imminent instability, with criticality reported from 0.78 up to just before the maximum load is reached. This finding is consistent with the classical FBM and its critical signature of the crossover phenomenon in avalanches.

5 CASE STUDY 2: MEXICO MW8.2 EARTHQUAKE ON 7 SEPTEMBER 2017

5.1 Study area and seismic data

This case study applies the precursor parameters from Section 3 to the seismicity preceding the Chiapas earthquake Mw8.2 of 7 September 2017, which struck at 04:49 UTC on the Cocos plate subducting beneath the North American and Caribbean plates. According to the National Seismological Service (SSN), the epicenter was in Gulf of Tehuantepec, 133 km southwest of Pijijiapan (14.761º N, -94.103º W; depth 45.9 km), associated with a normal fault. Seismic data

from the SSN catalog (www.ssn.unam.mx) from January 1, 1988 to September 7, 2017, were used, with a completeness magnitude of 3.5. The analyzed region includes Baja California, Chiapas, Colima, Guerrero, Jalisco, Michoacán and Oaxaca, comprising 55,723 events.

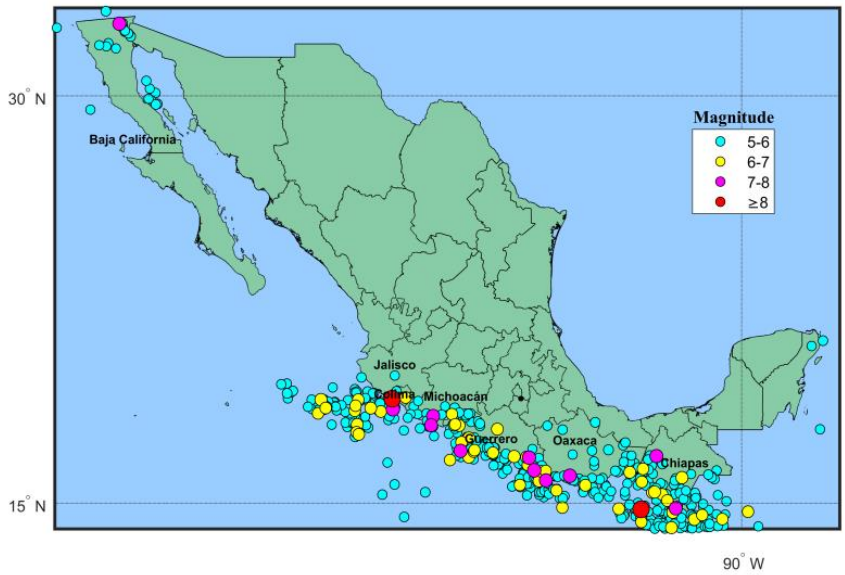

Figure 3. Spatial distribution of seismic events with magnitude ≥6 in Mexico. The analyzed region includes the states of Baja California, Colima, Jalisco, Michoacán, Guerrero, Oaxaca, and Chiapas.

5.2 Results and discussion

Fig. 4(a) illustrates the seismic activity and the cumulative number of earthquakes. Along the Pacific coast of Mexico, seismicity is characterized by frequent large-magnitude events (Mw 5–7). The sole occurrence of an Mw 8 event, apart from the primary shock, transpired on October 9, 1995.

Fig. 4(b) presents the *b*-value confidence interval. The analysis used a 150-event sliding window with a 250-event step size. This methodological decision ensures statistical robustness, as a single day may include 50-100 events, thereby proving representative samples and a clear temporal evolution. In the early stages (Mw 6-8) exhibit constrained confidence intervals and mean *b*-values of ~0.8-1.9 (normalized time 0.3-0.5), reflecting system stability. Approaching the mainshock (normalized time 0.7-1.0), larger fluctuations and wider intervals indicate anomalous magnitude dispersion, consistent with a critical regime preceding the Mw8.2 earthquake.

The MCF-B approach was applied to the Mw8.2 Mexico EQ in Fig. 4(c). The exponents p_2 and p_3, obtained as in Case Study 1, reveal no clear critical signature: p_3 fluctuates toward negative values for most of the analyzed period, reflecting an upward tail in the N(A)–A relationship. This tail arises from large, isolated events that were recorded and are associated with intense seismic activity. Therefore, the *b*-value and its fluctuation prior to the main earthquake appear to be effective indicators of system instability.

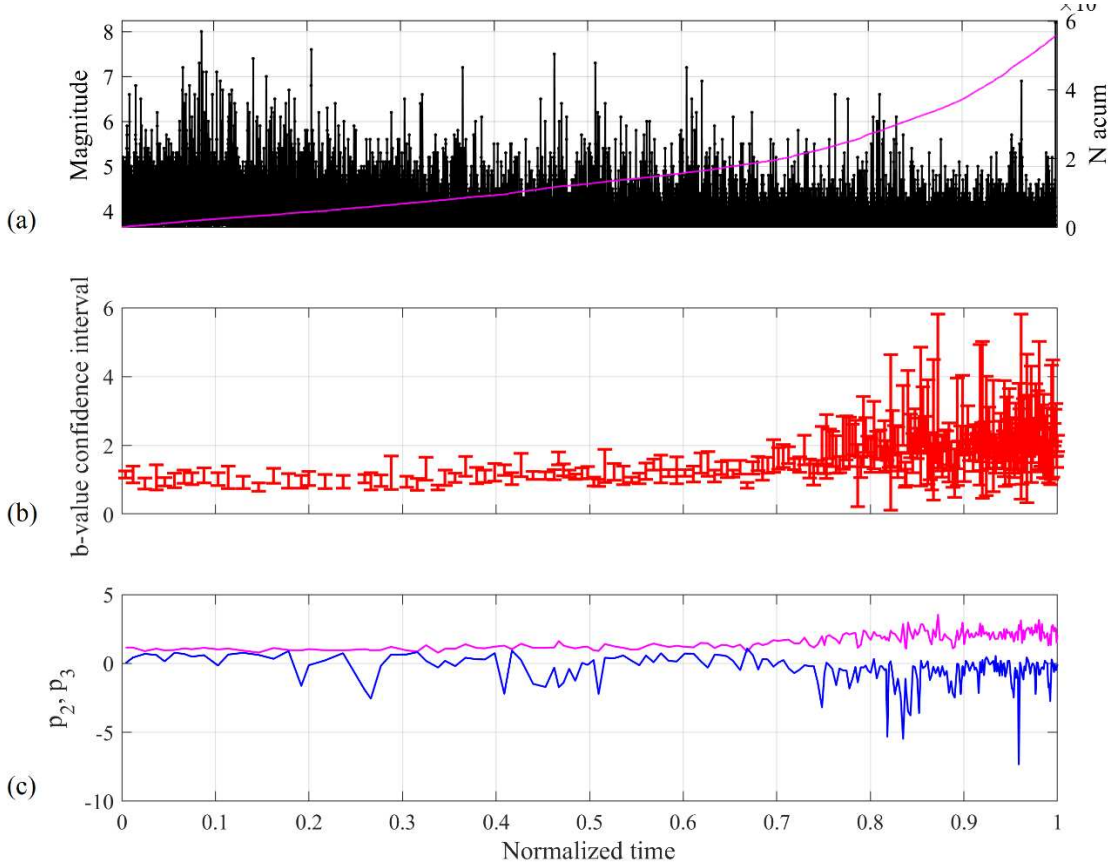

Figure 4. (a) The EQ magnitude's reported by SSN, accumulated number of EQs on the right-hand scale, (b) Confidence Interval of b-value analysis, (c) exponents p_2 and p_3 from the MCF-B approach. The horizontal axis is the normalized time and equal for (a)-(c).

As previously indicated, the region exhibits a high vulnerability to large-scale seismic events. Consequently, the MCF-B model appears to be somewhat inaccurate. In previous work, Friedrich et al. (2025) analyzed seismic data from the Kahramanmaras-Gazientep region in Turkey, from 2014 to 2023 (Figure 5(a)), and identified a clear critical signature prior to the mainshock, as shown in Fig. 5(b). The behavior of the p_2 and p_3 exponents can be illustrated in Fig. 5(c), with the N(A)–A distribution at different points throughout the analyzed period. Further investigation is necessary to determine the effectiveness of MCF-B. In subsequent studies, the data from the Chiapas region could be examined independently to discern the effects of the three tectonic plates present there. Additional seismic data could be incorporated for a more comprehensive investigation, using predictors from this study and new ones.

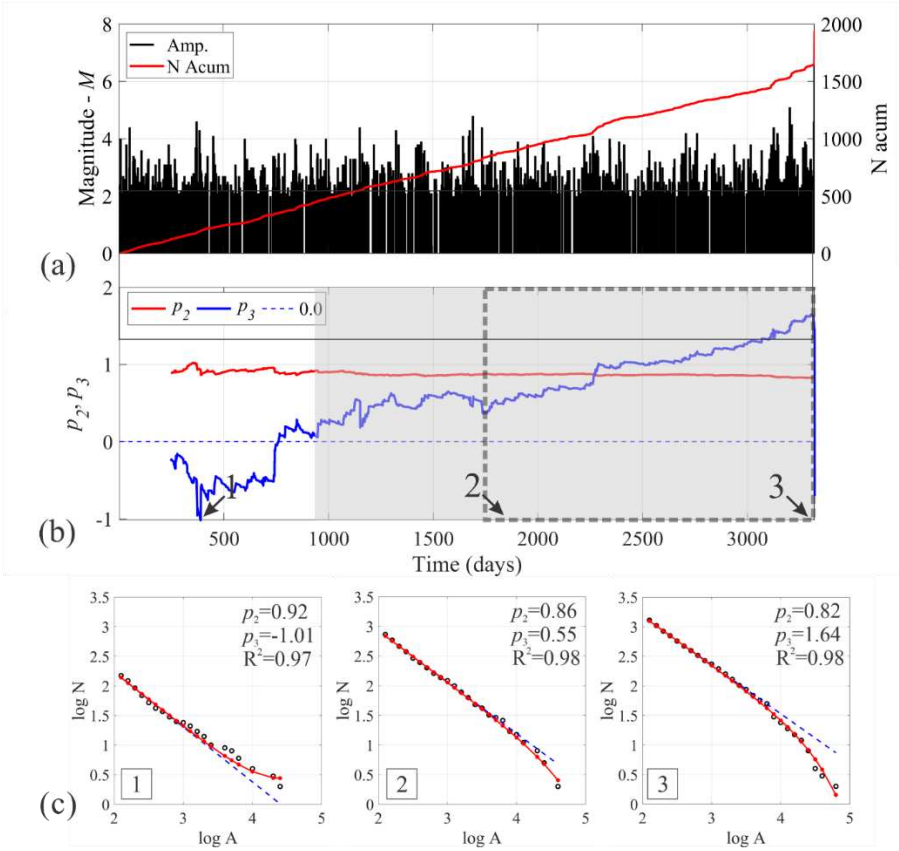

Figure 5. (a) The EQ magnitude's reported by AFAD, accumulated number of EQs on the right-hand scale, (b) exponents p_2 and p_3 from the MCF-B approach, the horizontal axis is in days up to the main shock and equal for (a) and (b); (c) evolution of exponents p_2 and p_3, together with the coefficient of determination R², for points 1, 2 and 3 indicated by black arrows in Fig. 5(b). The dotted blue line is the linear approximation.

5 CONCLUSIONS

This paper examines two approaches to identifying critical states in complex systems: the *b*-value and the MCF-B. The first case study is a fracture process monitored by AE derived from FBM simulations within the LDEM framework. The second case study is the time series of earthquakes preceding the devastating Mw8.2 event in Mexico (2017). In the simulation, the accumulated number of events and AE amplitudes indicate progressive damage leading to catastrophic failure. The *b*-value evolution and MCF-B exponents provide consistent critical signatures. The seismic case shows that *b*-value fluctuations effectively capture the transition to a critical regime, while the MCF-B approach failed to yield a robust signature due to the predominance of large, isolated events. This underscores the efficacy of *b*-value analysis as a reliable indicator of impeding instability. In contrast, the applicability of MCF-B may be context-dependent, requiring refinement for complex tectonic environments, such as the Mexico Pacific Coast. Future work should expand the dataset, incorporate regional differences, and test combined predictors to improve the reliability of seismic precursor identification.

Acknowledgments

The authors wish to acknowledge the support of the Brazilian National Council for Scientific and Technological Development (CNPq), the Coordination for the Improvement of Higher Education Personnel (CAPES), and the Research Support Foundation of the State of Rio Grande do Sul (FAPERGS), under grant numbers 22/2551-0000841-0 and 24/2551-0000772-5.

REFERENCES

Carpinteri, A., Lacidogna, G., Puzzi, S., From criticality to final collapse: Evolution of the "b-value" from 1.5 to 1.0. Chaos, Solitons, and Fractals, 41, 843—853, 2008. https://doi.org/10.1016/j.chaos.2008.04.010

Contoyiannis, Y.F., Diakonos, F.K., Criticality and intermittency in the order parameter space. *Physics Letters A*, 268, 286—292, 2000. https://doi.org/10.1016/S0375-9601(00)00180-8

Daniels, H. E., The statistical theory of the strength of bundles of threads, I. *Proceedings of the Royal Society a Mathematical, Physical and Engineering sciences*, 183, 405—435, 1945. https://doi.org/10.1098/rspa.1945.0011

Friedrich, L. F., Cezar, E. S., Colpo, A.B., Tanzi, B.N, Lacidogna, G., Iturrioz, I., Identifying impeding failure in heterogeneous materials: A study on acoustic emission time series. *Chaos, Solitons & Fractals*, 185, 2024 https://doi.org/10.1016/j.chaos.2024.115172

Friedrich, L. F., Padilha, M. H., Lacidogna, G., and Iturrioz, I., Multiscale investigation of seismic precursors before major earthquakes. *Mechanics Research Communications*, 147, 2025. https://doi.org/10.1016/j.mechrescom.2025.104449

Gutenberg, B., Richter, C.F., Seismicity of the earth and associated phenomena. Princeton University Press, 1949.

Hillerborg, A., A model for fracture analysis, Division of Building Materials LTH, Lund University. 3005, 1978.

Huang, M., Jiang, L., Liaw, P. K., Brooks, C. R., Seeley, R., and Klarstrom, D. L., Using Acoustic Emission in Fatigue and Fracture Materials Research. *JOM: The Journal of the Minerals*, 50, 1998.

Kosteski, L., Barrios D'Ambra, R., Iturrioz, I., Crack propagation in elastic solids using the truss-like discrete element method. *International Journal of Fracture*, 174, 139—161, 2012. https://doi.org/10.1007/s10704-012-9684-4

Kwapien, J., and Drozdz, S., Physical approach to complex systems. *Physics Reports*, 515, 115—226, 2012. https://doi.org/doi:10.1016/j.physrep.2012.01.007

Ladyman, J., Lambert, J., and Wiesner, K. What is a complex system? *European Journal for Philophy of Science,* 3:33–67, 2012. https://doi.org/10.1007/s13194-012-0056-8

Lei, X., Ma, S., Laboratory acoustic emission study for earthquake generation process. *Earthquake Science*, 27, 627—646, 2014. https://doi.org/10.1007/s11589-014-0103-y

Potirakis, S.M., Contoyiannis, Y., Schekotov, A., Eftaxias, K., and Hayakawa, M., Evidence of critical dynamics in various electromagnetic precursors. *The Euroupean Physical Journal Special Topics*, 230, 151—177, 2021. https://doi.org/10.1140/epjst/e2020-000249-x

Pradhan, S., Hansen, A., and Chakrabarti, B., Failure processes in elastic fiber bundles. Reviews of Modern Physics, 82, 499—555, 2010. https://doi.org/10.1103/RevModPhys.82.499

Pradhan, S., Hansen, A., Hemmer, Per., Crossover Behavior in Burst Avalanches: Signature of Imminent Failure. Phyisical Review Letters, 95, 2005. https://doi.org/10.1103/PhysRevLett.95.125501

Riera, J.D., Iturrioz, I., Discrete elements model for evaluating impact and impulsive response of reinforced concrete plates and shells subjected to impulsive loading. *Nuclear Engineering and Design*, 1791 135—144, 1998. https://doi.org/10.1016/S0029-5493(97)00270-7

Turcotte, D. L., and Malamud, B. D., Earthquakes as a Complex System. *International Geophysics*, 81A, 209—227, 2002. https://doi.org/10.1016/S0074-6142(02)80217-0